Growth instability in Cu multilayer films due to fast edge/corner diffusion

Yunsic Shim* and Jacques G. Amar†
Department of Physics & Astronomy, University of Toledo, Toledo, Ohio 43606, USA
(Received 11 July 2005; revised manuscript received 6 December 2005; published 20 January 2006)

The instability observed in Cu/Cu(100) epitaxial growth by Ernst *et al.* [Phys. Rev. Lett. **72**, 112 (1994)] is studied using serial kinetic Monte Carlo (KMC) simulations as well as a recently proposed algorithm for parallel KMC. Our parallel algorithm allows us to simulate longer time scales which are not easily accessible by a serial Monte Carlo simulation. Two different sets of activation barriers were used—one based on effective medium theory and the other based on the embedded-atom method. In both cases, we find that the existence of very fast edge diffusion along close-packed step edges along with a slight enhancement of the rate of corner diffusion is crucial to explaining the experimental results. Some possible mechanisms for this enhancement are discussed.

DOI: 10.1103/PhysRevB.73.035423 PACS number(s): 81.15.Aa, 68.55.−a, 81.10.Aj

I. INTRODUCTION

The formation of mound structures during unstable epitaxial growth has drawn much attention both experimentally[1–9] and theoretically.[10–19] The growth instability in homoepitaxial growth arises from the existence of diffusion bias which leads to an uphill current toward ascending step edges and an increased probability for the nucleation of islands on top of existing islands. One important cause of diffusion bias is the existence of an Ehrlich-Schwoebel (ES) barrier to interlayer diffusion.[20] Another possible cause is the short-range attraction of diffusing terrace atoms to surface steps.[16]

Recently a number of other processes have also been shown to be important. For example, it has been shown[13–15] that edge diffusion may also lead to an uphill surface current and thus contribute to a growth instability. Recent work[21,22] also indicates that in the presence of an Ehrlich-Schwoebel barrier,[20] the short-range attraction of depositing atoms to step edges may also play an important role. In particular, molecular-dynamics simulations of adatom deposition near step edges on metal (100) and (111) surfaces[21,22] indicate that the short-range attraction of depositing atoms to steps can lead to significant deviations from the standard downhill funneling[23] (DF) picture. In the presence of an ES barrier such an effect can significantly enhance the mound instability as well as the selected mound slope.

In recent experiments on unstable Cu/Cu(100) growth at low temperatures, Ernst *et al.*[1] observed a dramatic change in the roughening behavior as the temperature was increased. In these experiments the growth exponent β (where $w \sim \langle h \rangle^{\beta}$, w is the rms surface height or surface roughness, and $\langle h \rangle$ is the average film height) was measured at two different temperatures. At $T=160$ K, mounds with (113) facets were observed with a growth exponent $\beta \simeq 0.26$. However, at $T=200$ K, the surface roughness and growth exponent ($\beta \simeq 0.56$) were significantly larger although the mound slope was lower. By including the effects of the short-range attraction of depositing atoms to steps in their kinetic Monte Carlo (KMC) simulations of Cu/Cu(100) growth along with energy barriers based on effective-medium theory (EMT), Yu and Amar[21] obtained excellent agreement with the experimental results at 160 K. However, this same model leads to poor agreement with experiment at 200 K. In addition, due to the existence of very fast edge diffusion at 200 K, such simulations are very slow and time consuming. As a result, typically the rate of edge diffusion is artificially reduced to speed up the simulation.

Here we propose that the existence of very fast edge diffusion in Cu/Cu(100) is crucial to explaining the experimental behavior. In particular, we find that by including the full edge diffusion in our simulations along with a slight enhancement of the rate of corner diffusion, the rapid change in the growth exponent with increasing temperature from $\beta=0.25$ at 160 K to $\beta=0.56$ at 200 K observed experimentally, can be explained. The resulting fast edge and corner diffusion leads to an uphill current which increases with film thickness due to mound coarsening, and thus to a growth exponent $\beta \simeq 0.5$ and an increasing mound angle.

In order to test the model dependence of our results, our simulations were carried out using two different sets of energy barriers—one based on effective medium theory (EMT) and the other based on the embedded-atom method (EAM). In both cases, we find that the existence of very fast edge diffusion along close-packed step edges along with a slight enhancement of the rate of corner diffusion is crucial to explaining the experimental results. We note that to speed up our simulations without artificially reducing the rate of edge diffusion we have used our recently developed synchronous sublattice algorithm for parallel kinetic Monte Carlo.[24] We have also studied the dependence of our results on the rate of edge diffusion. These results should be useful in carrying out large scale simulations of processes with very fast events in the future.

The organization of this paper is as follows. In Sec. II we first describe our growth model including the two different sets of energy barriers used. In Sec. III we present our simulation results and compare with experimental results at 160 and 200 K. The dependence on the ES barrier, rate of corner diffusion, and rate of edge diffusion are also discussed. We

also discuss the similarities and differences between the EMT and EAM barrier results. Finally, in Sec. IV we summarize our results.

II. MODEL AND SIMULATIONS

In our simulations we have used two different models with two different sets of energy barriers—one obtained from effective medium theory (EMT) and the other set obtained using the embedded atom method (EAM). In both cases the fcc crystalline geometry was taken into account[21,25] by including an amount of "uphill funneling" equivalent to that obtained in previous molecular-dynamics simulations[21] of the deposition of Cu atoms near close-packed step edges. We note that in KMC simulations with the usual DF and no short-range attraction, atoms are assumed to be deposited only at the underlying fcc(100) lattice sites, each of which corresponds to a "capture zone" for deposition.[25,26] In particular, if a selected deposition site is a fourfold hollow site, then the deposited atom remains where it is immediately after deposition. However, if one or more of the fourfold hollow "support" atoms is missing, then the atom "cascades" randomly to one of the missing support sites. This process is repeated until a fourfold hollow site is found. Thus the probability that an atom deposited beyond a close-packed [110] step edge arrives at the upper terrace is given by $P_{up}=0$. In the simulations presented here, the deposition process is similar, but with a small modification to take into account the effects of uphill funneling as determined from molecular-dynamics simulations.[21] In particular, if an atom lands at a site which is not a fourfold hollow site but for which one or more of the missing support sites are themselves fourfold hollow sites, then one of these fourfold hollow sites is randomly selected. Otherwise, the deposition process is the same as for DF. This leads to a probability $P_{up}=1/2$ that an atom deposited in a window of width $a_1/2$ (where a_1 is the nearest-neighbor distance) beyond a close-packed step edge arrives at the upper terrace, in good agreement with molecular-dynamics simulations.

A. Effective-medium theory (EMT) model

The EMT model used in our simulations corresponds to a parametrization of the EMT barriers calculated by Jacobsen.[27] As already noted this model was previously used[21] along with uphill funneling as described above and a minimal ES barrier to obtain excellent quantitative agreement with the Ernst *et al.*[1] experimental results for surface roughening in Cu/Cu(100) growth at $T=160$ K. As shown in Fig. 1(a), in this model the energy barriers for hopping of an adatom on a flat terrace are determined by interactions with five of the eight neighboring atoms. In particular if an adatom (filled circle) has a lateral bond with neighboring site i (where $i=A$, B_1, B_2, C_1, and C_2) then the occupation number N_i for that site is 1 and otherwise it is 0. The energy barrier E_{barr} for hopping may then be calculated using the expression[27]

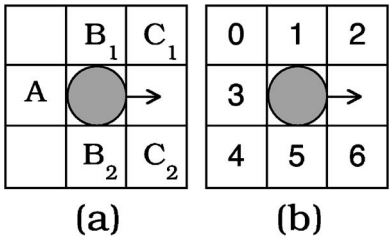

FIG. 1. Schematic diagram showing neighboring atoms affecting the energy barrier of a diffusing atom (filled circle) in (a) EMT and (b) EAM models.

$$E_{\mathrm{barr}} = E_a + \frac{E_a}{2}[\delta(N_A,1) - 1 + \delta(N_{C_1},0)\delta(N_{C_2},0)(1+\delta(N_{B_1},1)\delta(N_{B_2},1))], \quad (1)$$

where $E_a=0.425$ eV is the activation energy for monomer diffusion. Once the activation barrier is obtained, the rate for a given move is given by $D=D_0\, e^{-E_{barr}/k_BT}$. As indicated by Eq. (1), in this model the barrier for edge diffusion ($E_e \simeq 0.21$ eV) is much lower than that for monomer diffusion ($E_a=0.425$ eV) while the effective rate for dimer diffusion is essentially the same as for monomer diffusion. The barrier for detachment from a corner site in a direction parallel to the edge ($E_d \simeq 0.425$ eV, see Fig. 2) is the same as for monomer diffusion. We note that once an atom has detached from a corner site, the barrier to reattach (either to the same corner site or to the other corner site) is significantly lower, e.g., $E_{att} \simeq 0.21$ eV. Thus the effective barrier for corner diffusion in this model is $E_c \simeq 0.425$ eV.

In order to obtain an appropriate prefactor D_0, the antiphase diffraction factor at a coverage of 0.3 monolayer (ML) at $T=213$ K and deposition rate $F=0.1$ ML/min was calculated for different values of D_0 and compared with the corresponding experimental results of Swan *et al.*[28] We note that this deposition rate is sufficiently fast that effects such as dimer shearing[28,29] do not play a role in submonolayer growth. Using this method, a value of $D_0=3\times10^{11}$ sec^{-1} was obtained.

B. Embedded atom method (EAM) model

In order to compare with our EMT model results, we have also performed KMC simulations with an entirely different set of energy barriers[30,31] obtained using the embedded atom

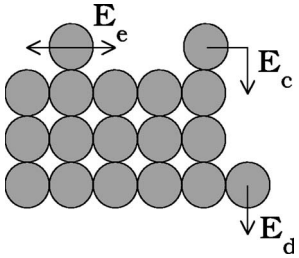

FIG. 2. Schematic diagram showing edge and corner diffusion with activation barriers E_e and E_c, respectively, along with corner detachment barrier E_d.

TABLE I. Comparison between EMT and EAM values for energy barriers for edge diffusion E_e, monomer diffusion E_a, and corner detachment E_d. The values of the EMT energy barriers in parentheses are given for comparison for the prefactor $D_0=10^{13}\text{sec}^{-1}$.

	E_e (eV)	E_a (eV)	E_d (eV)	D_0 (sec^{-1})
EMT	0.21 (0.27)	0.425 (0.485)	0.42-0.64	3×10^{11} (10^{13})
EAM	~0.24	0.48	0.54-0.89	10^{13}

method (EAM). We note that in simulations[32] of Cu/Cu(100) submonolayer growth using this model, excellent agreement was found with experimental results for the island separation over approximately two orders of magnitude in the deposition flux as well as over a range of temperatures ($T=213$ K–$T=263$ K). In this model the energy barriers for hopping on a flat terrace depend explicitly on all eight neighboring sites [see Fig. 1(b)]. In particular, they can be roughly categorized into four different groups: (i) monomer diffusion with energy barrier 0.48 eV, (ii) very fast edge-diffusion with energy barrier 0.24 eV, (iii) detachment from islands with barriers ranging from 0.54 to 0.89 eV, and (iv) very fast low barrier events such as island-edge attachment (0.01–0.13 eV). We note that this last category includes a number of very-low barrier repetitive moves in which an atom shuttles back and forth between two equivalent or approximately equivalent sites (e.g., the moves corresponding to $n_1=68$ and $n_2=34$, 35 and 48–51 in Ref. 31). Thus, in order to make the simulation feasible, we have introduced an energy barrier cutoff E_{cut} such that if $E_{barr}<E_{\text{cut}}$, then the energy barrier is replaced by the cutoff value. In preliminary simulations up to 5 ML at 200 K, the results were found to be independent of cutoff for $E_{cut}<0.2$ eV. Accordingly, in our 60-ML growth simulations a cutoff value $E_{\text{cut}}\simeq0.2$ eV was used. We also note that while the largest energy barriers in this model are significantly larger than for the EMT model, the prefactor $D_0=1.0\times10^{13}$ sec^{-1} is also significantly larger. As a result, even though the EAM model is significantly more complicated, the rates for monomer and dimer diffusion, edge diffusion, and corner detachment are roughly the same as for the EMT model over the temperature range considered here ($T=160$–200 K). Table I summarizes the key diffusion barriers for both models along with the corresponding prefactors. Also shown in parentheses are the equivalent EMT barriers using the same prefactor as for the EAM model.

C. Energy barriers for interlayer and corner diffusion

In growth on metal (100) surfaces, the ES barriers for interlayer diffusion at both close-packed [110] and open [100] step edges may play a role. We note that there have been a variety of estimates for the interlayer diffusion barrier E_{ES} at close-packed step edges[33–38] ranging from 0.03 eV (Ref. 33) to a more recent estimate of 0.18 eV.[38] However, in previous work using the EMT model at 160 K it was found[21] that due to the relatively low rate of monomer diffusion at this temperature, the results are relatively insensitive to the ES barrier. In contrast, due to the higher rate of monomer diffusion at 200 K, we expect that the results will depend sensitively on the value of the ES barrier at this temperature. Accordingly, we have carried out simulations using ES barriers ranging from 0.02 to 0.1 eV.

We also note that recent EMT calculations[37] indicate that the ES barrier at open [100] step edges may be significantly lower than at close-packed [110] step edges. However, for simplicity in most of our simulations we have assumed that the ES barriers for both types of step edges are the same. For comparison we have also carried out simulations in which the barrier at open step edges and kinks was significantly lower than at close-packed step edges. This led to results which were basically equivalent to those obtained using our simpler model but with a somehat smaller global ES barrier.

For both the EMT and EAM models, the rate of corner diffusion is determined by the activation barrier for detachment parallel to the edge at a corner ($E_d=0.425$ eV for EMT and $E_d=0.54$ eV for EAM, see Fig. 2). However, in our simulations we have slightly enhanced the effective rate of corner diffusion by introducing a corner-rounding move with activation barrier E_c (see Fig. 2). This enhanced corner-rounding move is only allowed to occur in the case of in-plane motion, i.e., no combined corner-rounding and interlayer diffusion moves are included in our simulations. The dependence of the results on the corner-rounding rate was then studied (see Fig. 4). We note that in most of the results presented here the "corner-rounding" move was suppressed for dimers and trimers since this leads to enhanced dimer and trimer diffusion. However, for comparison we have also carried out simulations in which dimer and trimer diffusion due to corner diffusion was included. While this led to mounds which were somewhat more uniform in size than in the absence of dimer and trimer diffusion, only a negligible difference in the surface roughness was observed.

D. Parallel and serial simulations

In order to speed up our simulations, which are extremely time consuming[39] due to the existence of rapid low-barrier events such as edge diffusion at 200 K, we have carried out both parallel and serial simulations. In our parallel simulations we have used our recently developed semirigorous synchronous sublattice (SL) algorithm for parallel kinetic Monte Carlo simulations of thin-film growth.[24] In this algorithm different parts of the system are assigned via spatial decomposition to different processors. However, in order to avoid conflicts between processors due to the synchronous nature of the algorithm, each processor's domain is further divided into different regions or sublattices. Each processor simultaneously and independently carries out KMC events in a randomly selected sublattice until the time of the next event exceeds a fixed time interval I_T corresponding to the average time for the fastest possible activated event. For the EMT model, $I_T=1/D_e$ where D_e is the rate of edge diffusion, while for the EAM model $I_T=1/D_{\text{cut}}$.

In both our parallel and serial KMC simulations we used a fixed system size $L=256$ along with a deposition rate $F=1/120$ ML/s corresponding to that used in the Ernst *et al.*[1] experiments. Due to the relatively small system size, only four processors were used in our parallel simulations.

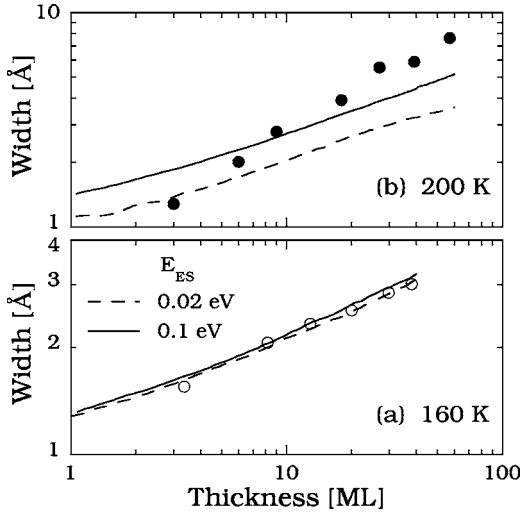

FIG. 3. Surface width vs film thickness for EMT model without enhanced corner diffusion for two different values of the ES barrier along with experimental results (circles) at (a) $T=160$ K and (b) $T=200$ K.

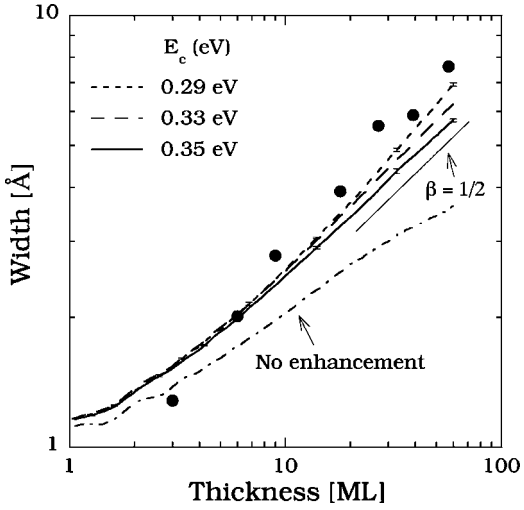

FIG. 4. Surface width vs film thickness for three different values of the corner diffusion barrier E_c along with experimental results (filled circles) at $T=200$ K. Here the EMT model is used with $E_{ES}=0.02$ eV.

For the EMT model without enhanced corner diffusion a parallel efficiency of 60% was obtained, while in the presence of enhanced corner diffusion the parallel efficiency was somewhat lower. In addition, since the parallel efficiency for this algorithm tends to decrease as the time interval I_T is decreased, the EAM model parallel simulations were less efficient than the EMT model simulations. As already noted, due to the existence of rapid edge diffusion at 200 K even our parallel simulations are quite time consuming.[39] Accordingly, our results were typically averaged over only five runs. However, due to the relatively large system size used in our simulations, the error bars were found to be quite small (see Figs. 4, 6–8, and 10). We note that for clarity, error bars are only shown for a few selected points.

III. RESULTS

Figure 3 shows our results for the rms surface width as a function of film thickness for values of the ES barrier ranging from 0.02 to 0.1 eV for the EMT model in the absence of enhanced corner diffusion. Results are shown at both 160 and 200 K along with the corresponding experimental results of Ernst *et al.*[1] As can be seen, at 160 K there is excellent agreement between the simulation results and experiment. In addition, as previously observed[21] there is only a very weak dependence on the ES barrier at this temperature. However, the simulation results at 200 K do not agree with the corresponding experimental results as shown in Fig. 3. In particular, the measured growth exponent $\beta=0.36\pm0.01$ for the case of $E_{ES}=0.1$ eV and coverage $\theta>10$ ML is significantly smaller than the experimentally measured value $\beta=0.56$. Similar results (not shown) have also been obtained for the EAM model. Thus while increasing the ES barrier leads to increased surface roughness at 200 K, it is not sufficient to explain the experimentally observed behavior.

These results suggest the possible existence of an additional diffusion mechanism operating in Cu/Cu(100) growth which is not included in our models. As already noted, one possibility we have considered is the existence of enhanced corner diffusion with a diffusion barrier $E_c<E_d$ where E_d is the activation barrier for detachment at a corner. Figure 4 shows the surface width as a function of film thickness for the EMT model at 200 K both with and without enhanced corner diffusion. Results are shown for different values of the corner diffusion barrier E_c ranging from 0.29 to 0.35 eV, while a relatively weak Ehrlich-Schwoebel barrier $E_{ES}=0.02$ eV has been assumed. As can be seen, as the rate of corner diffusion is increased the growth exponent β increases and approaches the experimentally observed behavior. We note that the largest corner diffusion barrier ($E_c=0.35$ eV) corresponds to a relatively small enhancement in the rate of corner diffusion as well as a relatively small shift (approximately 0.07 eV) from the EMT prediction $E_d\simeq0.42$ eV for the barrier for detachment at a corner. Accordingly, in simulations at 160 K with $E_c=0.35$ eV, good agreement was found with the corresponding experimental results. In contrast, simulations at 160 K with smaller corner diffusion barriers ($E_c=0.29$ eV and $E_c=0.33$ eV) resulted in significant deviations from the experimental results. Accordingly, in the rest of our EMT model simulations, enhanced corner diffusion has been included with a value $E_c=0.35$ eV.

Figure 5 shows a comparison of the mound morphology at 200 K with and without enhanced corner diffusion after 20 MLs have been deposited. As can be seen, in the case of enhanced corner diffusion the mounds are somewhat larger and more regular. Also shown [Fig. 5(c)] is the case in which enhanced corner diffusion for dimers and trimers has been included. While the surface roughness in this case is the same as without dimer or trimer diffusion, the mounds are somewhat more uniform in size and better ordered.

We now consider the dependence of the surface roughness on the ES barrier for the EMT model with enhanced corner diffusion ($E_c=0.35$ eV). As shown in Fig. 6, the surface

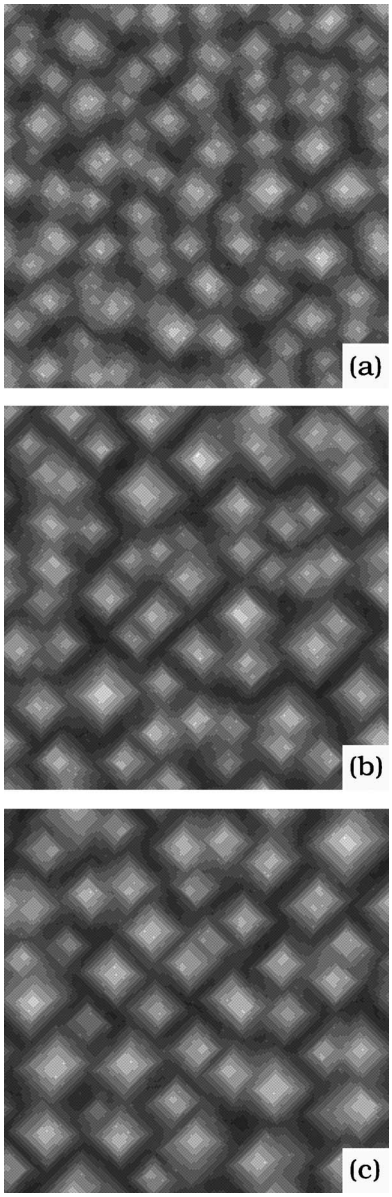

FIG. 5. Surface mound morphology at $T=200$ K after 20 layers have been deposited for EMT model with $E_{ES}=0.02$ eV (a) without corner diffusion, (b) enhanced corner diffusion with $E_c=0.35$ eV, (c) same as (b) but with dimer and trimer corner diffusion allowed.

roughness increases as the ES barrier increases. However, the growth exponent $\beta \simeq 1/2$ for $\theta > 10$ ML is essentially independent of the ES barrier and is in good agreement with the observed experimental behavior. In particular, a fit to the EMT data for $\theta > 10$ MLs and $E_{ES}=0.02$ eV gives $\beta=0.48\pm0.01$. We note that for a larger ES barrier ($E_{ES}=0.1$ eV) there is reasonably good quantitative agreement with experiment for coverages above 10 MLs while for a smaller ES barrier ($E_{ES} \simeq 0.02$ eV) the surface roughness is significantly lower. However, in all cases the low-coverage behavior is somewhat different from experiment.

For comparison, we have also carried out EAM model simulations with enhanced corner diffusion with a corner diffusion barrier ($E_c=0.42$ eV) corresponding to the same overall rate of corner diffusion as in the EMT model. Figure 7 shows a summary of our results for both the EMT and EAM models with enhanced corner diffusion at 160 and 200 K along with the corresponding experimental results (circles). The EMT model results are shown for both a relatively weak ES barrier (solid curve, $E_{ES}=0.02$ eV) as well as for a larger barrier (dashed curve, $E_{ES}=0.1$ eV) while for the EAM model only the results with a weak ES barrier are shown. As can be seen, the inclusion of enhanced corner diffusion leads to semiquantitative agreement with experiment for both the EAM and EMT models at 200 K as well as good agreement at 160 K. We also note that for the same ES barrier there is not much difference between the results for the EAM and EMT models.

We now consider the nature of the transition in the roughening behavior observed in our simulations with enhanced

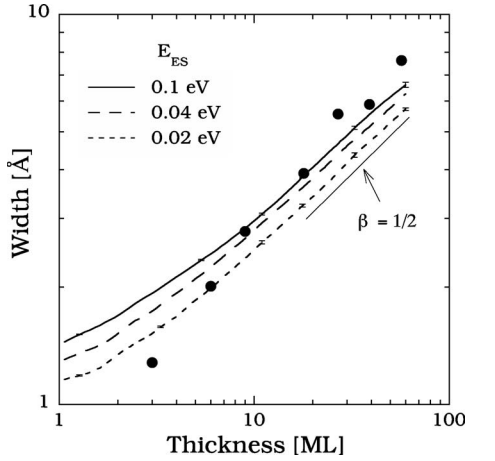

FIG. 6. Surface width vs film thickness for EMT model with enhanced corner diffusion ($E_c=0.35$ eV) for three different values of the ES barrier along with experimental results (filled circles) at $T=200$ K. Straight line with slope 1/2 is guide to the eye.

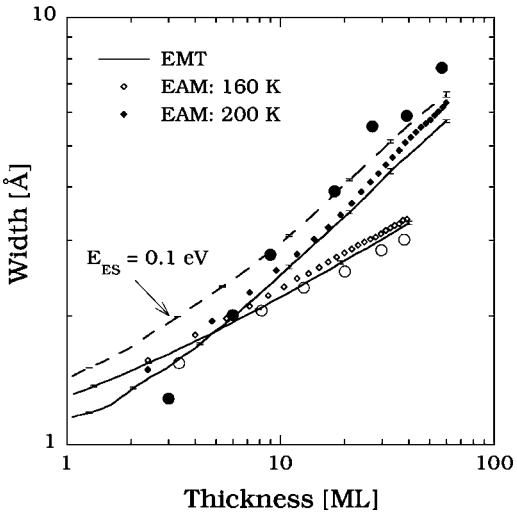

FIG. 7. Surface width vs film thickness for EMT and EAM models with enhanced corner diffusion at 160 and 200 K along with experimental results (circles). Solid lines and symbols correspond to $E_{ES}=0.02$ eV while dashed line corresponds to EMT model with $E_{ES}=0.1$ eV.

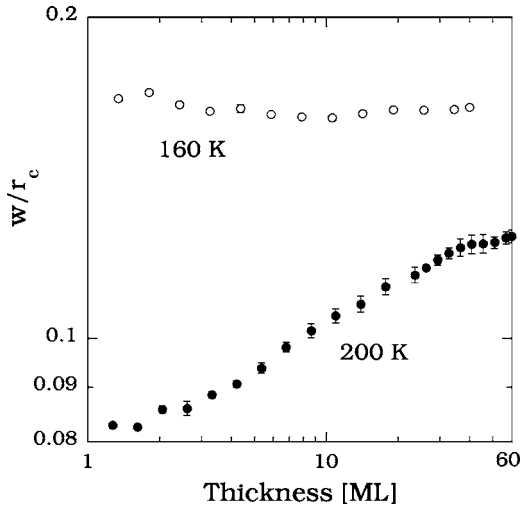

FIG. 8. Mound angle ratio as function of film thickness for EMT model with $E_{ES}=0.02$ eV and enhanced corner diffusion at $T=160$ and 200 K.

corner diffusion as the temperature is increased from 160 to 200 K. In previous work it has been shown[18] that while unstable mound growth leads to a growth exponent $\beta=1/4$ in the presence of slope selection, a much larger value $\beta\simeq 1/2$ may occur in the absence of slope selection. In order to test for the presence of slope selection in our simulations, we have measured the mound angle ratio w/r_c of the surface width w to the correlation length r_c (where the correlation length or mound size r_c is determined from the zero crossing of the circularly averaged height-height correlation function[4]). Figure 8 shows our results for w/r_c as a function of film thickness at both 160 and 200 K for the EMT model with enhanced corner diffusion. As can be seen, at 160 K the mound-angle ratio is independent of film thickness which is consistent with the experimentally observed growth exponent $\beta\simeq 1/4$. On the other hand, the observed increase in w/r_c with film thickness in our 200 K simulation results indicates that the slope is not selected in this case and is consistent with the large growth exponent $\beta\simeq 1/2$ observed at this temperature. We note that the mound-angle ratio is also smaller at 200 K than at 160 K, in qualitative agreement with the experimental observation of smaller angle facets at 200 K than at 160 K.

IV. DISCUSSION

We have carried out extensive simulations of Cu/Cu(100) growth using both EMT and EAM models. By including a slight enhancement of the rate of corner rounding beyond that predicted by the EMT and EAM models, we have obtained reasonably good agreement with the experimental results of Ernst *et al.*[1] for the dependence of the surface roughness on film thickness at 160 and 200 K. In particular, our simulations lead to a rapid increase in the growth exponent from $\beta\simeq 1/4$ at 160 K to $\beta\simeq 1/2$ at 200 K in agreement with experimental observations. The inclusion of enhanced corner diffusion also leads to semiquantitative agreement with experiment for the surface roughness at 200 K as well as preserving the excellent quantitative agreement at 160 K. We note that the reduction in the corner-rounding barrier used in our EMT simulations (approximately 0.07 eV) is relatively small relative to the EMT prediction for the barrier for detachment at a corner. Accordingly, the barrier for corner rounding is still significantly larger than that for edge diffusion and thus our model still predicts a relatively large kink Ehrlich-Schwoebel effect (KESE) barrier for corner diffusion. This is consistent with previous simulations[38] of step-flow growth of Cu/Cu(100) in which fast edge diffusion with a large KESE barrier was assumed and good qualitative agreement with experiment was observed.

It is worth noting that in models without a downhill current due to deposition near step edges, the resulting lack of slope selection can also lead to qualitative behavior (e.g., $\beta\simeq 1/2$) similar to that observed for Cu/Cu(100) growth at 200 K. However, such an absence of downhill current is not consistent with molecular-dynamics simulation results for deposition at step edges[21] or with the experimental observation of a selected slope at 160 K. We also note that if the ratio D/F of the monomer diffusion rate D to the deposition flux F is sufficiently large[25] (e.g., $D/F>10^7$) then even in the presence of a downhill current at step edges, an extended period of growth may occur during which the mound slope is increasing thus leading to a growth exponent $\beta\simeq 1/2$.[25] However, in Cu/Cu(100) growth at 200 K, the ratio $D/F\simeq 10^3$–10^4 is much too small for such a scenario to hold, while the rate of edge diffusion is much larger ($D_e/F\simeq 10^8$).

In contrast, our results suggest that it is the existence of extremely fast diffusion along close-packed step edges, coupled with a sufficiently rapid rate of corner rounding, which plays a crucial role in explaining the observed behavior at 200 K. In particular, we expect that the fast edge diffusion with enhanced corner diffusion leads to a large uphill surface current[13] which enhances the surface roughness and mound instability. As the mounds coarsen with increasing film thickness, the distance over which edge atoms may diffuse also increases, thus further enhancing the uphill surface current. It is this increase in the uphill surface current with film thickness which leads to the increase in mound slope and large roughness exponent at 200 K.

To understand this better, we have also studied the dependence of our results on the rate of edge diffusion along close-packed step edges. One of the motivations for this is that artificially reducing this rate may be an excellent strategy to reduce the simulation time, since for a sufficiently large rate of edge diffusion, one expects that the results should be independent of diffusion rate. Figure 9 shows a comparison between results obtained for the EMT model with enhanced corner diffusion with $E_c=0.35$ eV at 200 K for different rates of edge diffusion $D_e'=RD_e$ where the reduction factor R ranges from 0.001 to 1. We note that for the range of values shown, the simulation time is proportional to R, thus indicating that edge diffusion is the dominant process in the system. As can be seen, for a reduction factor which is not too small

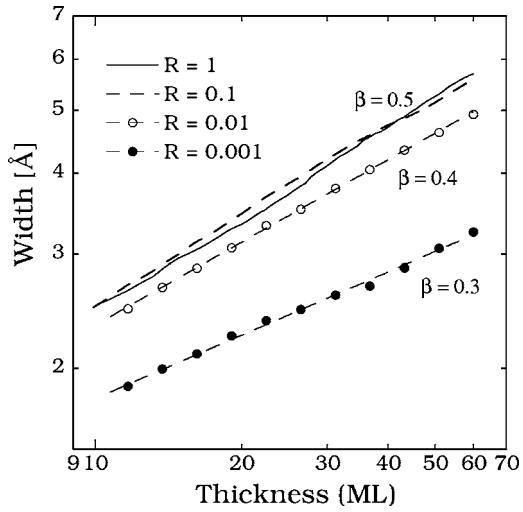

FIG. 9. Log-log plot of surface roughness vs film thickness for EMT model with enhanced corner diffusion (E_c=0.35 eV) and E_{ES}=0.02 eV at 200 K for different values of edge-diffusion reduction factor R.

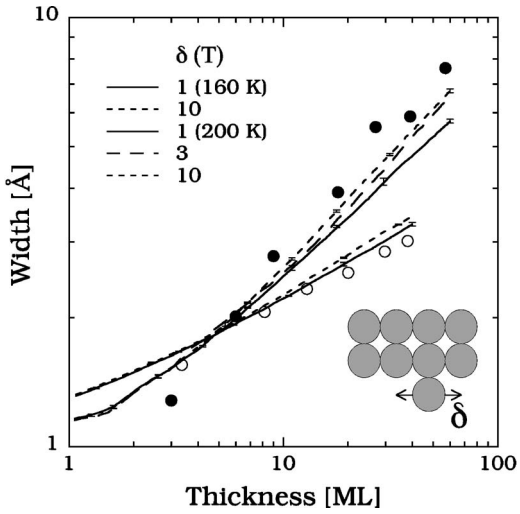

FIG. 10. Surface width vs film thickness for different values of corner attraction ratio δ at 160 and 200 K for EMT model with enhanced corner diffusion (E_c=0.35 eV) and E_{ES}=0.02 eV along with experimental results (circles). The inset shows a schematic diagram of the edge atom one step away from a corner site.

(e.g., $0.1 \leqslant R \leqslant 1$) the surface roughness is effectively independent of the reduction factor R. However, for a smaller reduction factor $R \leqslant 0.01$, both the surface roughness and the growth exponent β deviate significantly from the results obtained with full edge diffusion.

As a more sensitive test of the reduction-factor dependence, we have also measured the submonolayer island-size distribution at temperature T=200 K. In this case we find that even for R=0.1, there is a small but noticeable difference in the results obtained with a reduction factor and the corresponding results obtained without any reduction factor. Thus even a relatively small reduction factor can affect the results obtained in the early stages of growth.

We now consider the enhancement of the corner-diffusion rate which was included in our simulations. A key question is the origin of such enhanced corner diffusion. One possibility is that the barrier for detachment at corner sites is indeed somewhat less than the value predicted by the EMT and EAM models. However, another possibility is that some more complex collective mechanism such as exchange at corners may lead to a somewhat lower barrier for corner rounding. As an example, EAM calculations by Shi *et al.*[29] and Mehl *et al.*[31] indicate the existence of relatively low barriers ranging from 0.37 to 0.43 eV for collective processes such as dimer shearing along and towards a step edge. These barriers are comparable to and even lower than the value E_c=0.42 eV assumed in our EAM model simulations with enhanced corner rounding. In contrast, the predicted barrier for the breakup of a tetramer via dimer shearing (0.69 eV) is significantly larger. Thus it is possible that such collective processes may lead to an enhancement of the effective rate of corner rounding in Cu/Cu(100) growth but without altering the submonolayer growth. Such dimer-shearing processes have been ignored in previous simulations of Cu/Cu(100) submonolayer growth[31] because it was believed that their main effect was to slightly modify the island morphology but not to otherwise modify the growth.

It is also interesting to compare our simulation results with those obtained for Ag/Ag(100) for which the rate of diffusion along close-packed step edges is also expected to be very high. In simulations of Ag/Ag(100) growth[40–42] good agreement with experiment was obtained by including a kink-rounding barrier which was significantly lower than that predicted by EAM calculations.[43] However, in these simulations "global" corner rounding (e.g., corner rounding at corners other than kinks) was not allowed. In contrast, in our simulations we have made no distinction between corner rounding at kinks and at global corners. In order to compare with these simulations we have also carried out simulations with enhanced corner rounding at kinks but without enhanced global corner rounding. However, this led to results which were essentially the same as in the absence of enhanced corner diffusion. Thus the enhancement of corner rounding at global corners appears to be essential to explain our results. Since this can significantly enhance the surface current, such a result is consistent with our assumption that it is the enhancement of the surface current due to edge and corner diffusion which is essential to explain the experimental results.

Finally, we note that there exists another effect corresponding to the attraction of edge atoms to corners, which may also enhance the effective rate of corner rounding. In particular, one may define the quantity δ as the ratio of the rate for an atom one step away from a corner site to hop towards the corner divided by the rate to hop away from the corner (see inset of Fig. 10). In recent EAM calculations,[44] the difference in the corresponding barriers was found to be $\Delta E \simeq 0.02$ eV,[44] which implies $\delta \simeq 3$ at T=200 K. A somewhat weaker effect has also been observed previously in EAM calculations for Ag/Ag(100).[43] Figure 10 shows simulation results obtained using our EMT model with corner attraction as well as enhanced corner diffusion at both 160

and 200 K. As can be seen, while there is very little effect at 160 K, corner attraction leads to a significant increase in the surface roughness as well as a slight increase in the growth exponent at 200 K. This indicates that corner attraction may also play an important role in enhancing the surface roughness in experiment.

ACKNOWLEDGMENTS

This research was supported by the NSF through Grant Nos. DMR-0219328 and CCF-0428826. We would also like to acknowledge grants of computer time from the Ohio Supercomputer Center (Grant No. PJS0245).

*Electronic address: yshim@physics.utoledo.edu
†Electronic address: jamar@physics.utoledo.edu

[1] H.-J. Ernst, F. Fabre, R. Folkerts, and J. Lapujoulade, Phys. Rev. Lett. **72**, 112 (1994).
[2] M. D. Johnson, C. Orme, A. W. Hunt, D. Graff, J. Sudijono, L. M. Sander, and B. G. Orr, Phys. Rev. Lett. **72**, 116 (1994).
[3] K. Thürmer, R. Koch, M. Weber, and K. H. Rieder, Phys. Rev. Lett. **75**, 1767 (1995).
[4] J. A. Stroscio, D. T. Pierce, M. D. Stiles, A. Zangwill, and L. M. Sander, Phys. Rev. Lett. **75**, 4246 (1995).
[5] J. E. Van Nostrand, S. J. Chey, M.-A. Hasan, D. G. Cahill, and J. E. Greene, Phys. Rev. Lett. **74**, 1127 (1995).
[6] F. Tsui, J. Wellman, C. Uher, and R. Clarke, Phys. Rev. Lett. **76**, 3164 (1996).
[7] L. C. Jorritsma, M. Bijnagte, G. Rosenfeld, and B. Poelsema, Phys. Rev. Lett. **78**, 911 (1997).
[8] J.-K. Zuo and J. F. Wendelken, Phys. Rev. Lett. **78**, 2791 (1997).
[9] R. Gerlach, T. Maroutian, L. Douillard, D. Martinotti, and H.-J. Ernst, Surf. Sci. **480**, 97 (2001).
[10] J. Villain, J. Phys. I **1**, 19 (1991).
[11] M. Siegert and M. Plischke, Phys. Rev. Lett. **73**, 1517 (1994); M. Siegert, *ibid.* **81**, 5481 (1998).
[12] M. Siegert and M. Plischke, Phys. Rev. E **53**, 307 (1996).
[13] M. V. Ramana Murty and B. H. Cooper, Phys. Rev. Lett. **83**, 352 (1999).
[14] O. Pierre-Louis, M. R. D'Orsogna, and T. L. Einstein, Phys. Rev. Lett. **82**, 3661 (1999).
[15] M. V. Ramana Murty and B. H. Cooper, Surf. Sci. **539**, 91 (2003).
[16] J. G. Amar and F. Family, Phys. Rev. Lett. **77**, 4584 (1996).
[17] J. G. Amar, Phys. Rev. B **60**, R11317 (1999).
[18] L. Golubovic, Phys. Rev. Lett. **78**, 90 (1997).
[19] P. Smilauer and D. D. Vvedensky, Phys. Rev. B **52**, 14263 (1995).
[20] G. Ehrlich and F. G. Hudda, J. Chem. Phys. **44**, 1039 (1966); R. L. Schwoebel, J. Appl. Phys. **40**, 614 (1969).
[21] J. Yu and J. G. Amar, Phys. Rev. Lett. **89**, 286103 (2002).
[22] J. Yu and J. G. Amar, Phys. Rev. B **69**, 045426 (2004); J. Yu, J. G. Amar, and A. Bogicevic, *ibid.* **69**, 113406 (2004).
[23] J. W. Evans, D. E. Sanders, P. A. Thiel, and A. E. DePristo, Phys. Rev. B **41**, R5410 (1990).
[24] Y. Shim and J. G. Amar, Phys. Rev. B **71**, 125432 (2005).
[25] J. G. Amar and F. Family, Phys. Rev. B **54**, 14742 (1996).
[26] M. C. Bartelt and J. W. Evans, Phys. Rev. Lett. **75**, 4250 (1995).
[27] J. Jacobsen (unpublished); T. L. Einstein, J. Jacobsen, and C. Schiff, Bull. Am. Phys. Soc. **42**, 26 (1997).
[28] A. K. Swan, Z.-P. Shi, J. F. Wendelken, and Z. Zhang, Surf. Sci. **391**, L1205 (1997).
[29] Z.-P. Shi, Z. Zhang, A. K. Swan, and J. F. Wendelken, Phys. Rev. Lett. **76**, 4927 (1996).
[30] O. Biham, I. Furman, M. Karimi, G. Vidali, R. Kennett, and H. Zeng, Surf. Sci. **400**, 29 (1998).
[31] H. Mehl, O. Biham, I. Furman, and M. Karimi, Phys. Rev. B **60**, 2106 (1999).
[32] I. Furman, O. Biham, J.-K. Zuo, A. K. Swan, and J. F. Wendelken, Phys. Rev. B **62**, R10649 (2000).
[33] M. Karimi, T. Tomkowski, G. Vidali, and O. Biham, Phys. Rev. B **52**, 5364 (1995).
[34] C.-L. Liu, Surf. Sci. **316**, 294 (1994).
[35] O. S. Trushin, K. Kokko, P. T. Salo, W. Hergert, and M. Kotrla, Phys. Rev. B **56**, 12135 (1997).
[36] Z. Wang, Y. Li, and J. B. Adams, Surf. Sci. **450**, 51 (2000).
[37] J. Merikoski, I. Vattulainen, J. Heinonen, and T. Ala-Nissila, Surf. Sci. **387**, 167 (1997).
[38] M. Rusanen, I. T. Koponen, J. Heinonen, and T. Ala-Nissila, Phys. Rev. Lett. **86**, 5317 (2001).
[39] Depending on the rate of corner diffusion, a single serial simulation using the EMT model of 60 ML of growth at 200 K can take from ten days to two weeks.
[40] K. J. Caspersen, C. R. Stoldt, A. R. Layson, M. C. Bartelt, P. A. Theil, and J. W. Evans, Phys. Rev. B **63**, 085401 (2001).
[41] K. J. Caspersen, A. R. Layson, C. R. Stoldt, V. Fournee, P. A. Thiel, and J. W. Evans, Phys. Rev. B **65**, 193407 (2002).
[42] P. A. Thiel and J. W. Evans, J. Phys. Chem. B **108**, 14428 (2004).
[43] A. F. Voter, Proc. SPIE **821**, 214 (1987).
[44] A. Karim, A. Kara, and T. S. Rahman (private communication).